AJNR

Volumetric Analysis of the Germinal Matrix and Lateral Ventricles Performed Using MR Images of Postmortem Fetuses

Yoshimasa Kinoshita, Toshio Okudera, Eichi Tsuru and Akira Yokota

This information is current as of May 6, 2025.

Volumetric Analysis of the Germinal Matrix and Lateral Ventricles Performed Using MR Images of Postmortem Fetuses

Yoshimasa Kinoshita, Toshio Okudera, Eichi Tsuru, and Akira Yokota

BACKGROUND AND PURPOSE: **The volumetric changes of the ventricular system and germinal matrix are important to understand brain maturation and the mechanism of subependymal hemorrhage. Our purpose was to show the 3D configuration of the brain, germinal matrix, and lateral ventricles and to discuss the volumetric changes of each structure with maturation by using high-resolution MR imaging.**

METHODS: **Three-dimensional MR images of 13 formalin-fixed fetal brains ranging from 7 to 28 weeks' gestational age (GA) were obtained on a 4.7-T unit. Each 3D configuration of the brain surface, germinal matrix, and ventricles was rendered from the cross-sectional imaging data sets and its volume measured.**

RESULTS: **The germinal matrix was detected on MR images at 9 weeks' GA. Its volume exponentially increased by 23 weeks' GA (maximum, 2346 mm³) and then sharply decreased at 28 weeks' GA. The volume of the lateral ventricles increased gradually and reached 2646 mm³ peak volume at 23 weeks' GA. Between 11 and 23 weeks' GA, total brain and germinal matrix volumes were exponentially increasing, but the volume ratio of germinal matrix to brain was stable at about 5%. On the other hand, the volume ratio of lateral ventricles to brain was large between 10 and 13 weeks' GA. This period corresponded to the lateral ventricle showing a "vesicular" aspect with a thin mantle, and the developing mantle thickness of the hemisphere resulted in the decreasing ratio.**

CONCLUSION: **Volumetric information concerning the germinal matrix and lateral ventricles may be useful in the accurate interpretation of clinical echograms and MR images of the fetal brain in utero.**

It is now possible to effectively examine the fetal brain by sonography, and, as a result, early diagnosis of intrauterine disorders has led to new management options (1–4). However, sonography has limitations involving resolution and contrast of inner structures. MR imaging has the advantage in this regard; however, it has been difficult to apply this technique in clinical studies because of fetal motion and altering positions. Recently, to decrease the influence of fetal movement on image quality

without sedation, faster imaging techniques have been applied to this clinical field, including the echo-planar technique (5), gradient-echo technique (6), fast spin-echo technique, and half-Fourier acquisition single-shot turbo spin-echo technique (7). Hansen et al (8) evaluated both preserved and fresh fetal specimens and concluded that formalin fixation does not significantly affect the appearance of anatomic structures. Although there are a few reports of postmortem MR studies of the fetal brain (9–12), there is no report of a volumetric study of the germinal matrix and lateral ventricles performed using high-resolution MR imaging. Moreover, the development of computer technology has opened new possibilities for 3D reconstruction. In this article, we show the 3D configuration of the brain, germinal matrix, and lateral ventricles and discuss the volumetric changes of each structure with maturation.

Methods

Thirteen legally aborted fetuses ranging from 7 to 28 weeks' gestational age (GA) were used in the study. Malformations

that were confirmed either in the CNS or on the surface of the body were excluded. GA was determined according to the chart developed by Shimamura (13) based on measurements of crown-rump length of the Japanese embryo and fetus, and expressed in the number of weeks from the first day of the last menstrual period. Each fetus was fixed for at least 3 months with neural formalin administered through an opening in the skull.

Embedding Method for 3D MR Imaging

It is difficult to set specimens in a small resonator without air contamination, morphologic changes caused by compression, or motion artifacts resulting from poor fixation. To avoid these artifacts, we embedded the formalin-fixed fetuses in alginate impression materials, Jeltrate Plus (Dentsply Limited, Konstantz, Germany), and set them into the resonator. This alginate is widely used to obtain negative impressions in odontotherapy. We prepared 7 g of Jeltrate Plus dissolved in 30 mL water to ensure adequate gelation time and hardness. The alginate impression material comprises irreversible hydrocolloids consisting of potassium alginate, and is a useful casting substance for MR measurements because of the absence of MR signal from this substance. This alginate impression allowed us to keep the formalin-fixed fetal head in an ideal position and to avoid susceptibility and motion artifacts.

Postmortem MR Imaging

MR measurements were performed using a SISCO/Varian MR imaging system (Spectroscopy Imaging Systems, Palo Alto, CA) with a 40-cm bore operating at a field strength of 4.7 T and equipped with an actively shielded gradient coil (1.8 G/cm). The hydrogen-1 resonance frequency was 200.43 MHz. MR images were obtained with a hand-made saddle type resonator (inner diameter, 4.6 cm) or with bird cage-type resonators (inner diameter, 8.9 or 16.5 cm), chosen according to the size of the fetal head. Multisectional images of the brain and 3D analyses of the brain and germinal matrix were obtained with a 3D steady-state free-precession (3D-SSFP) sequence. The 3D-SSFP sequence was performed with parameters of 200/9 (TR/TE), a flip angle of 90°, and four signals averaged per cycle for T1-weighted images. The field of view (FOV) was 30–100 × 30–100 mm with a 128 × 128 matrix, and the slab thickness was 30–100 mm with 128 partitions (the FOV and slab thickness were changed according to the size of the fetus). Each of 128 serial coronal, axial, and sagittal images was composed after 3D Fourier transformation.

After MR imaging, the background noise of the 2D slices was eliminated, relative optical density was normalized, and regions of interest were trimmed using the National Institutes of Health Image 1.59 software on a Macintosh computer (Apple Computer, Cupertino, CA). The cross-sectional imaging data sets were transferred to a workstation (Silicon Graphics Computer, Mountain View, CA) to render the brain surface, germinal matrix, and ventricles using Dr. View software (Asahi-Kasei Joho Systems Co., Tokyo). The volumes of the germinal matrix, lateral ventricles, and brain were measured on a workstation computer system.

Correlation of Postmortem MR Images and Hematoxylin-Eosin (H&E)-stained Sections

Three brains were used for the histopathologic examination. They were sectioned in coronal and sagittal blocks with a thickness of 2.5 mm each and dehydrated with ethanol beginning with a strength of 70% that was then increased to 80%, 90%, 95%, 97%, and finally to absolute ethanol for 2 days. Xylene was used as a clearing agent. Finally, the brain slices were embedded in paraffin. Owing to the shrinkage caused by 10% formalin fixation and by dehydration, clearance, and par-

affin wax embedding, macroscopic measurements of the right-left and superior-inferior diameters of the brains were performed before dehydration and after paraffin wax embedding, respectively. Paraffin-embedded brain tissues were cut coronally or sagittally in 8- to 10-μm slices, deparaffinized, and stained with H&E.

Results

Correlation of Postmortem MR Images and H&E-stained Sections

All photomicrographs of sagittal sections stained with H&E correlated well with 3D MR images of the fetal brain. The cortex and germinal matrix showed high signal intensity relative to white matter. The MR signal intensity correlation well with the cell density of the H&E-stained brain. The faint high-intensity layer in the white matter between the cortex and germinal matrix corresponded to the migrating neuroblast layer at 21 weeks' GA (Fig 1).

Correlation of MR Images and Macroscopic Brain Configuration

We found good correlation between the macroscopic brain and the 3D surface-rendered brain. The 3D surface-rendered brain was reconstructed from 2D images obtained in situ. On the other hand, because the macroscopic brain was excised from the skull, the photographs show deformity caused by gravity (Fig 2 upper and middle rows). Segmentation of the brain, germinal matrix, and lateral ventricles was done manually, and the 3D reconstruction of each segment was superimposed using a workstation. The germinal matrix was located ventrolateral to the lateral ventricles and extended along the lateral wall of the lateral ventricles (Fig 2, lower row). The 3D surface-rendered images showed the developmental changes in brain configuration, germinal matrix, and ventricular system (Fig 3). The cranial, cervical, and pontine flexures were formed at 7 weeks' GA. The pontine flexure caused the hindbrain roof to become quite thin. The lateral ventricles were large, with a thin mantle showing an embryonic aspect. At 9 to 11 weeks' GA, the hemispheres maintained their embryonic vesicular aspect with a thin wall and large ventricles. At 13 to 15 weeks' GA, the lateral ventricles were still large with a thin mantle showing a vesicular aspect. The corpus callosum was developed only anteriorly. At 17 weeks' GA, the cerebral mantle had increased in thickness, and the ventricular cavity of the frontal horn and body had decreased, but that of the trigone portion remained large. At 19 to 21 weeks' GA, with development of the corpus callosum, the frontal horn approached its adult form, but the posterior portion of the lateral ventricles remained large, with a bicornuate shape. At 23 to 25 weeks' GA, the ventricular cavity lessened anteriorly and the corpus callosum developed posteriorly, but the posterior horn was still large, with a fetal type configuration.

FIG 1. T1-weighted MR image (*left*) reconstructed from 3D-SSFP sequence and sagittal H&E-stained photomicrograph (*right*) of fetal brain at 21 weeks' GA. There is good correlation between the images. Each image reveals the germinal matrix (*arrows*) and migrating neuroblast layer (*arrowheads*).
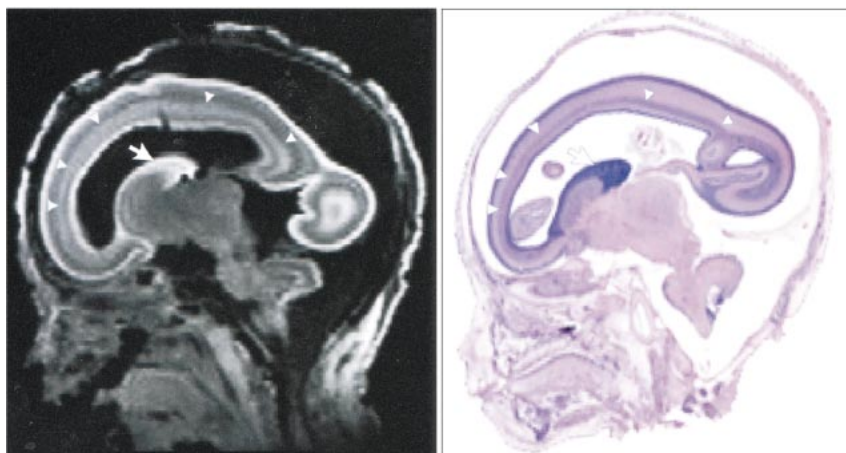

FIG 2. Images show good correlation between macroscopic brain (*upper row*) and 3D surface-rendered brain (*middle row*). Germinal matrix (*orange*), located ventrolateral to the lateral ventricles (*blue*), extends along the lateral walls of the lateral ventricles (*lower row*).

Operculization began, but the brain was agyric. At 28 weeks' GA, the configuration of the ventricular system approached its adult form, with a decrease in the cavity of the posterior horn and evidence of early gyral formation.

Brain Tissue Shrinkage by Paraffin Wax Embedding

Shrinkage caused by dehydration, clearance, and paraffin wax embedding did not differ significantly in the different directions on fetal coronal sections
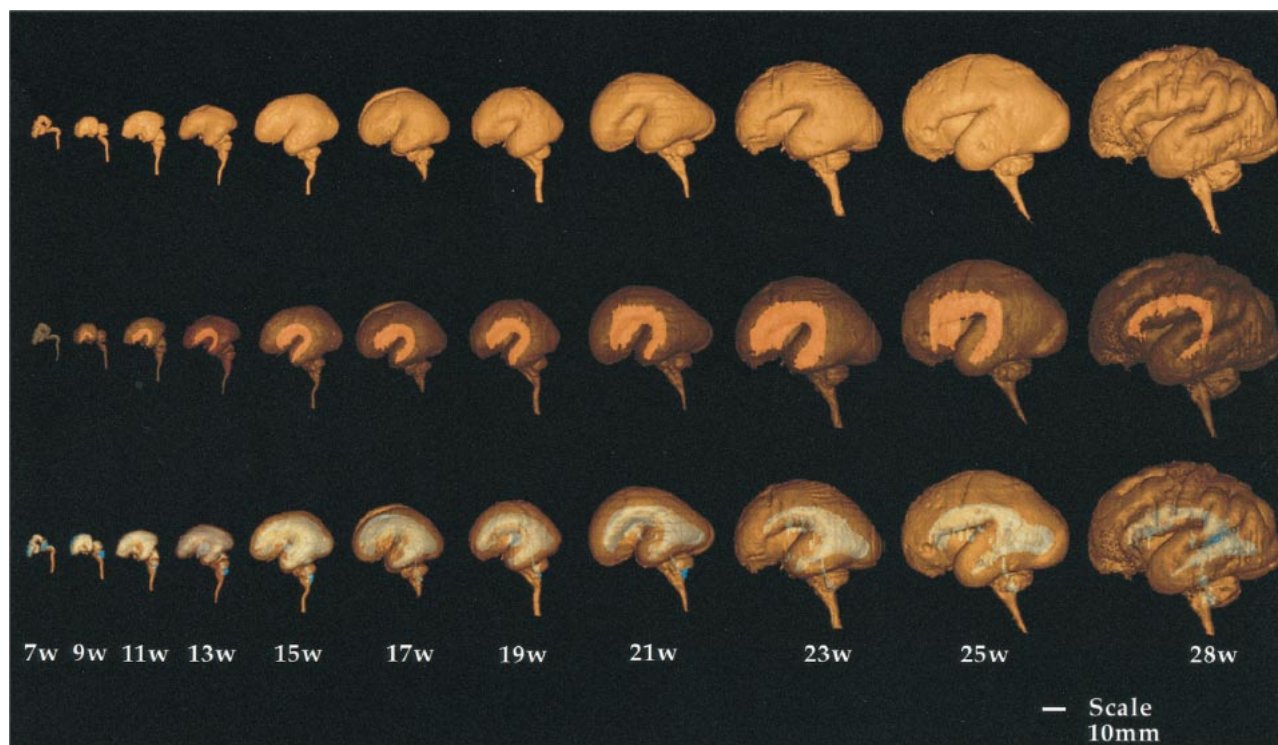
FIG 3. Successive images show developmental changes of lateral configuration of brain, germinal matrix, and ventricular system. The brain surfaces (*upper row*), germinal matrix (*middle row, orange*), and ventricular system (*lower row, blue*) of human fetal brain were reconstructed by surface rendering. The volume of the germinal matrix increased until 23 weeks' GA and decreased rapidly at 28 weeks' GA. Note how lateral ventricles change from fetal type, with vesicular aspect and bicornuate shape, to adult type with increasing GA.
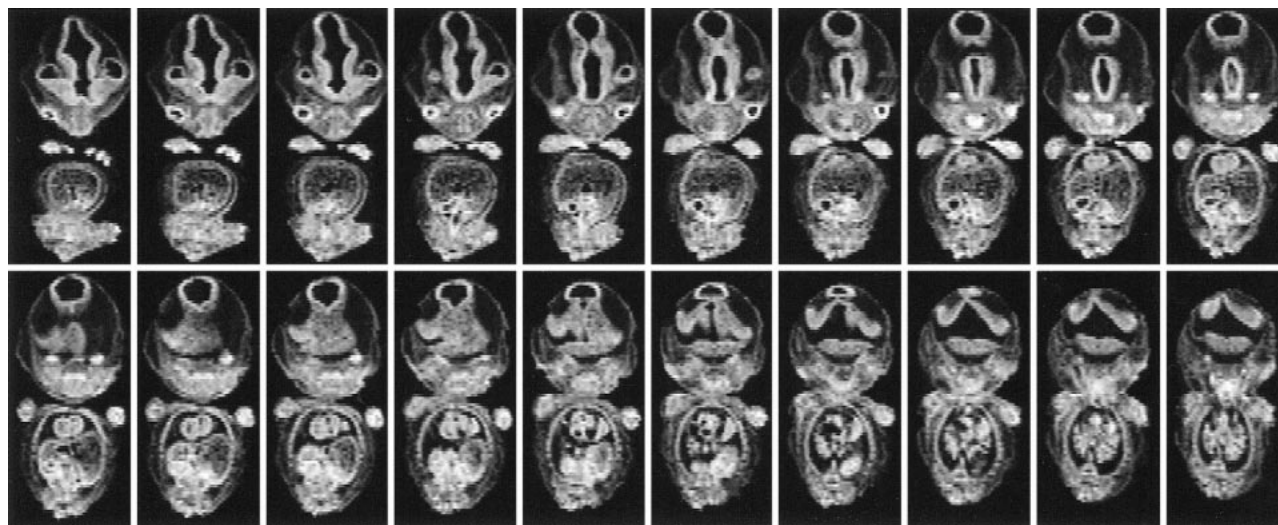

FIG 4. Serial coronal MR images of the fetus at 7 weeks' GA. Germinal matrix cannot be detected.

(right-left, $18.5 \pm 5.8\%$; superior-inferior, $16.2 \pm 4.3\%$). Paraffin wax embedding resulted in an average shrinkage of $17.1 \pm 4.4\%$ of the original dimension of a 10% formalin-fixed fetus.

Volumetric Study of the Brain, Germinal Matrix, and Lateral Ventricles

The germinal matrix could not be seen on MR images at 7 weeks' GA (Fig 4), but it was evident at 9 weeks' GA (Fig 5). The brain volume of the upper portion of the foramen magnum increased exponentially, reaching a volume of 132.5 cm^3 at 28 weeks' GA. An exponential relationship ($r^2 = .963$) was found between brain volume and GA (Fig 6). The germinal matrix increased exponentially, reaching a maximum volume of 2346 mm^3 at 23 weeks' GA, and its volume decreased rapidly after 25 weeks' GA. Although there was a large choroid plexus in the lateral ventricle, it was im-
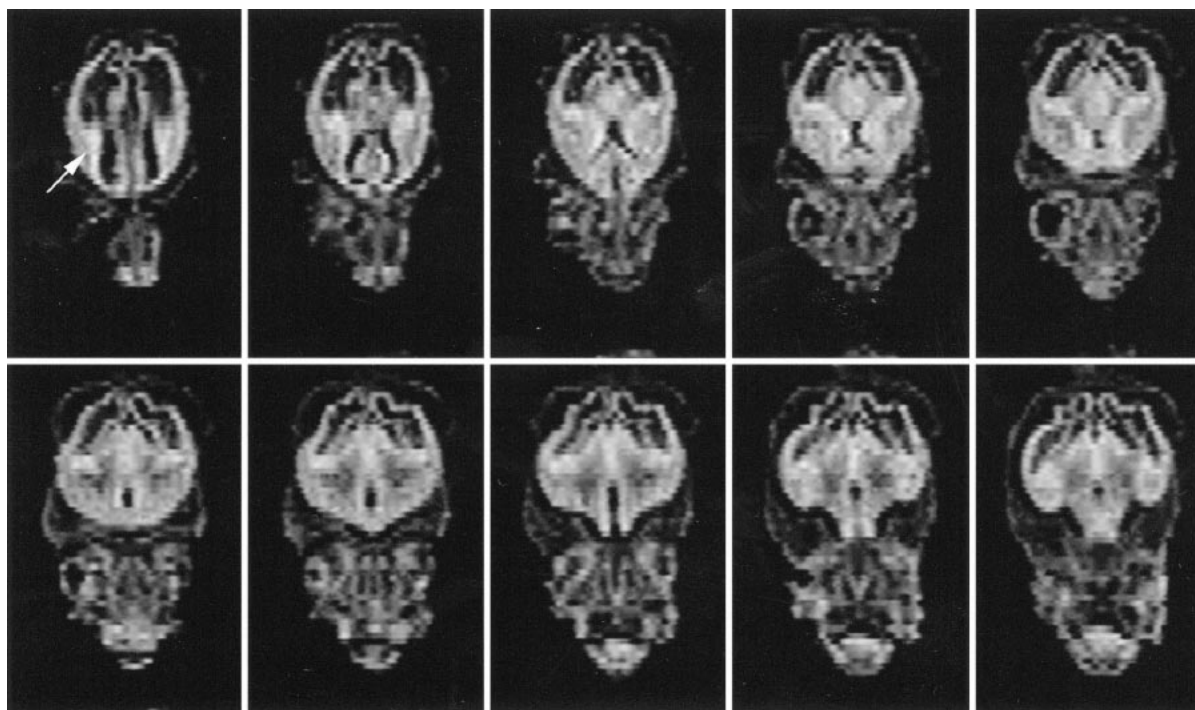
FIG 5. Serial coronal MR images of the fetus at 9 weeks' GA. Note germinal matrix is detected ventrolateral to the lateral ventricles (*arrow*).
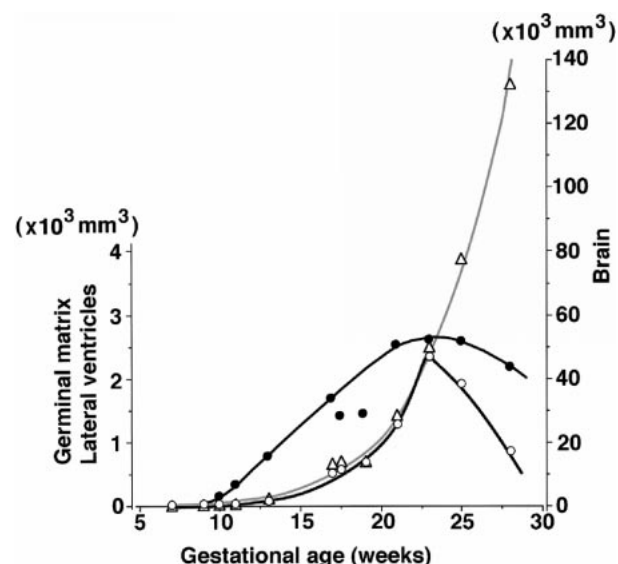

FIG 6. Volumetric changes of the fetal brain (*open triangles*), germinal matrix (*open circles*), and lateral ventricles (*solid circles*). Increasing fetal brain volume (*gray curve*) has an exponential relationship ($r^2 = .963$) to GA, reaching 132.5 cm³ at 28 weeks' GA. The germinal matrix also increases exponentially, reaching a volume of 2.3 cm³ at 23 weeks' GA, then decreases rapidly after 25 weeks' GA. In contrast to the germinal matrix, the volume of the lateral ventricles gradually increases, up to 2.6 cm³ at 23 weeks' GA.

possible to detect the choroid plexus on T1-weighted MR images because of its fine structure. Therefore, the volume of the lateral ventricles included the space of the CSF and choroid plexus. The volume of the lateral ventricles increased gradually

and reached a peak volume of 2646 mm³ at 23 weeks' GA (Fig 6).

Relationship between Germinal Matrix, Lateral Ventricles, and Brain

The volumes of both the brain and germinal matrix increased exponentially until 23 weeks' GA. The ratio of the volume of the germinal matrix to that of the brain was stable at about 5% between 11 and 23 weeks' GA and decreased to 0.7% at 28 weeks' GA, owing to the developing mantle thickness of the hemisphere (Fig 7). The ratio of the volume of the lateral ventricles to that of the brain increased between 10 and 13 weeks' GA, corresponding to the period in which the lateral ventricles showed a vesicular aspect with a thin mantle.

Discussion

This 3D MR analysis of the fetal brain has several advantages over traditional pathologic analysis. For one, it provides images of the fetal brain surface without having to excise the brain from the head, thus precluding artifacts accrued during excision and deformity produced by gravity. Second, arbitrary slices can be obtained from the 3D data set by postprocessing the images on a computer. Third, measurements of area and volume can be obtained for each component of the brain. Although the difference between fetal weight and volume is less than 2% (14), our estimates of fetal brain volume were similar to brain weights reported previously (15). Gong et al (16), who estimated
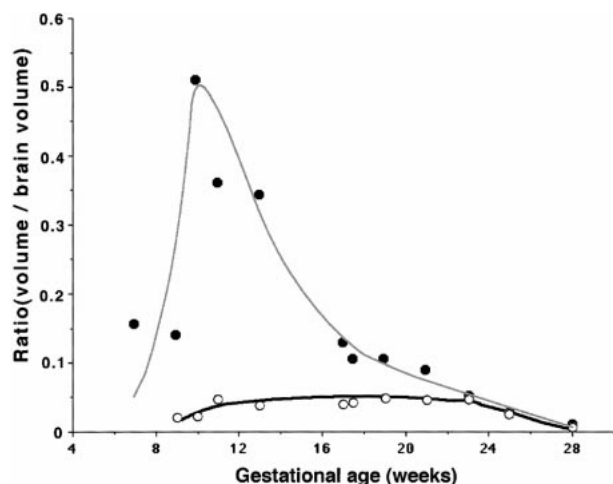
FIG 7.　Relationship between germinal matrix (*open circles*), lateral ventricles (*solid circles*), and brain. It is noteworthy that the volumetric ratio of the germinal matrix to brain volume is constant at about 5% between 11 and 23 weeks' GA.

fetal brain volume in the third trimester of pregnancy using gradient-echo in vivo MR imaging, suggested a linear relationship between fetal brain volume and GA. The brain volume at 28 weeks' GA was calculated as 154.2 mL by their equation, and that at the same age in our series was 132.5 cm^3. However, whereas Gong et al (16) found a linear increase in brain volume in the third trimester of pregnancy, our results showed an exponential increase in the second trimester.

Volumetric Analysis of the Germinal Matrix

Histopathologically, the germinal matrix has been detected at 7 weeks' GA (17), while in previous MR imaging studies it has been reported at 13 weeks' GA (10). In our study, the germinal matrix was detected on MR images at 9 weeks' GA. Only one previous report has described the volumetric changes in the germinal matrix by histopathologic study; we know of no report of such changes by MR imaging study. Jammes and Gilles (18) reported that the volume of the germinal matrix increased until 26 weeks' GA, reaching a half-hemispheric volume of about 400 to 580 mm^3, and then decreased rapidly after 27 weeks' GA. Our data showed similar volumetric changes, but the peak volume was quite different, reaching 2346 mm^3 in both hemispheres, or 1173 mm^3 for half the hemisphere. This discrepancy between histopathologic and 3D MR imaging volumetric measurements may be attributed to shrinkage of the samples. The shrinkage rate of pathologic specimens has been reported at 12.6% for the uterine cervix (19) and at 14.5% for a prostatic tumor (20). Shrinkage rates differ with the method of fixation and process of dehydration used. With our process of gradual dehydration, from 70% to 97% ethanol, terminating with absolute ethanol over a period of 2 days, the average shrinkage of the formalin-fixed

fetal brain after dehydration, clearance, and paraffin wax embedding was 17.1%. Shrinkage rates also depend on the water content of the brain tissue. The decreasing amount of water during development probably accounts for the discrepancy in our data, as the water content of the brain represents 90% to 91% of the total fresh weight in fetuses 10 to 34 weeks' GA, 88% to 89% at full term, 86% to 87% at 3 to 4 months, 80% at 6 months, and 72% at 2 years (21). In our experience, the shrinkage rate of the fetal brain is greater than 13.4% compared with the adult rat brain and 13.1% compared with the canine brain. The shrinkage rate of the nonmyelinated immature brain, which contains water-rich tissue, would be greater than that of mature brain. Thus, these shrinkage rates should be taken into account in any discussion of the volume of the nonmyelinated brain as determined from histopathologic specimens.

In our study, linear tissue shrinkage was 17.1% in each direction, for a net overall shrinkage volume (volumetric shrinkage) of $1-(0.829)^3$, or 43%. This degree of shrinkage, in turn, translates into a correction factor for tissue shrinkage of 1.76. Although standard histotechnological references clearly indicate that aqueous fixatives, such as formalin, cause minimal tissue shrinkage, we did not take into account the shrinkage rate caused by formalin fixation, because it has been reported to be only 2.7% (19) to 3.5% (20), which is smaller than that caused by dehydration, clearance, and paraffin wax embedding. Our volumetric study of the germinal matrix is the first to yield accurate measurements, and it is noteworthy that a constant volume ratio of germinal matrix (about 5%) to brain volume was maintained from 11 to 23 weeks' GA, while brain volume increased exponentially.

Volumetric Analysis of the Lateral Ventricles

There has been no report of a volumetric analysis of the ventricular system using ultraspeed MR imaging, although sonography has been applied to the analysis of ventricular configuration and volume. Blaas et al (22) used sonography to analyze fetal ventricular size in the first trimester, but their results differed from our findings of a crown-rump length of less than 40 mm. These authors used a 7.5-MHz annular array 3D transvaginal probe that had an axial resolution of 0.4 mm and a lateral resolution of 0.8 mm. On the other hand, the resolution in all directions on MR images was 0.23 mm for fetus with a crown-rump length of 21 mm, and 0.31 mm for fetuses with a crown-rump length of less than 45 mm. The sonographic measurement of lateral ventricles might be overestimated because the medial surface shows a complicated configuration of the hippocampal formation before 19 weeks' GA with development of the corpus callosum.

The volume ratio of lateral ventricles to brain increased between 10 and 13 weeks' GA, corre-

sponding to the vesicular period of the ventricular system. The exponentially increasing mantle thickness of the hemisphere after 15 weeks' GA generated the decreasing volume ratio of lateral ventricles to brain.

Conclusion

Our 3D MR analysis of postmortem fetal brains reveals the volumetric development of the germinal matrix and ventricles for the first time. With this information, it may be possible to understand the developmental process of the germinal matrix and ventricles during intrauterine life.

Acknowledgment

References

1. McGahan JP, Phillips HE. **Ultrasonic evaluation of the size of the trigone of the fetal ventricle.** *J Ultrasound Med* 1983;2:315–319
2. Pasto ME, Kurtz AB. **Ultrasonography of the normal fetal brain.** *Neuroradiology* 1986;28:380–385
3. Pilu G, De PL, Romero R, Bovicelli L, Hobbins JC. **The fetal subarachnoid cisterns: an ultrasound study with report of a case of congenital communicating hydrocephalus.** *J Ultrasound Med* 1986;5:365–372
4. Yagel S, Palti Z, Hurwitz A. **Detailed sonographic mappings of normal fetal brain anatomy in utero at six levels in the axial plain.** *Am J Perinatol* 1985;2:134–137
5. Johnson IR, Stehling MK, Blamire AM, et al. **Study of internal structure of the human fetus in utero by echo-planar magnetic resonance imaging.** *Am J Obstet Gynecol* 1990;163:601–607
6. Yamashita Y, Namimoto T, Abe Y, et al. **MR imaging of the fetus by a HASTE sequence.** *AJR Am J Roentgenol* 1997;168:513–519
7. Garden AS, Weindling AM, Griffiths RD, Martin PA. **Fast-scan magnetic resonance imaging of fetal anomalies.** *Br J Obstet Gynaecol* 1991;98:1217–1222
8. Hansen PE, Ballesteros MC, Soila K, Garcia L, Howard JM. **MR imaging of the developing human brain, 1: prenatal development.** *Radiographics* 1993;13:21–36
9. Brisse H, Fallet C, Sebag G, Nessmann C, Blot P, Hassan M. **Supratentorial parenchyma in the developing fetal brain: in vitro MR study with histologic comparison.** *AJNR Am J Neuroradiol* 1997;18:1491–1497
10. Chong BW, Babcook CJ, Salamat MS, Nemzek W, Kroeker D, Ellis WG. **A magnetic resonance template for normal neuronal migration in the fetus.** *Neurosurgery* 1996;39:110–116
11. Kier EL, Fulbright RK, Bronen RA. **Limbic lobe embryology and anatomy: dissection and MR of the medial surface of the fetal cerebral hemisphere.** *AJNR Am J Neuroradiol* 1995;16:1847–1853
12. Mintz MC, Grossman RI, Isaacson G, et al. **MR imaging of fetal brain.** *J Comput Assist Tomogr* 1987;11:120–123
13. Shimamura A. **Age determination and physical measurements of Japanese embryo.** *Jpn J Legal Med* 1957;11:795–811
14. Meban C. **The surface area and volume of the human fetus.** *J Anat* 1983;137:217–278
15. Ban T. **Studies on fetal brains of Japanese, IV: on the growth of the cerebrum and brain weight.** *Handai-Ishi* 1951;3:73–88
16. Gong QY, Roberts N, Garden AS, Whitehouse GH. **Fetal and fetal brain volume estimation in the third trimester of human pregnancy using gradient echo MR imaging.** *Magn Reson Imaging* 1998;16:235–240
17. Larroche JC. **The marginal layer in the neocortex of a 7-week-old human embryo.** *Anat Embryol* 1981;162:301–312
18. Jammes JL, Gilles FH. **Telencephalic development: matrix volume and isocortex and allocortex surface areas.** In: Gilles FH, Leviton A, Dooling EC, eds. *The Developing Human Brain.* Boston: John Wright;1983:117–183
19. Boonstra H, Oosterhuis JW, Oosterhuis AM, Fleuren GJ. **Cervical tissue shrinkage by formaldehyde fixation, paraffin wax embedding, section cutting and mounting.** *Virchows Arch A Pathol Anat Histopathol* 1983;402:195–201
20. Schned AR, Wheeler KJ, Hodorowski CA, et al. **Tissue-shrinkage correction factor in the calculation of prostate cancer volume.** *Am J Surg Pathol* 1996;20;1501–1506
21. Vanier MTH. *Contribution à l'Étude des Lipides Cérébraux au Cours du Developpementchez le Foetus et le Jeune Enfant.* Lyon, France: University of Lyon; 1974. Thesis
22. Blaas HG, Eik NS, Berg S, Torp H. **In-vivo three-dimensional ultrasound reconstructions of embryos and early fetuses.** *Lancet* 1998;352:1182–1186